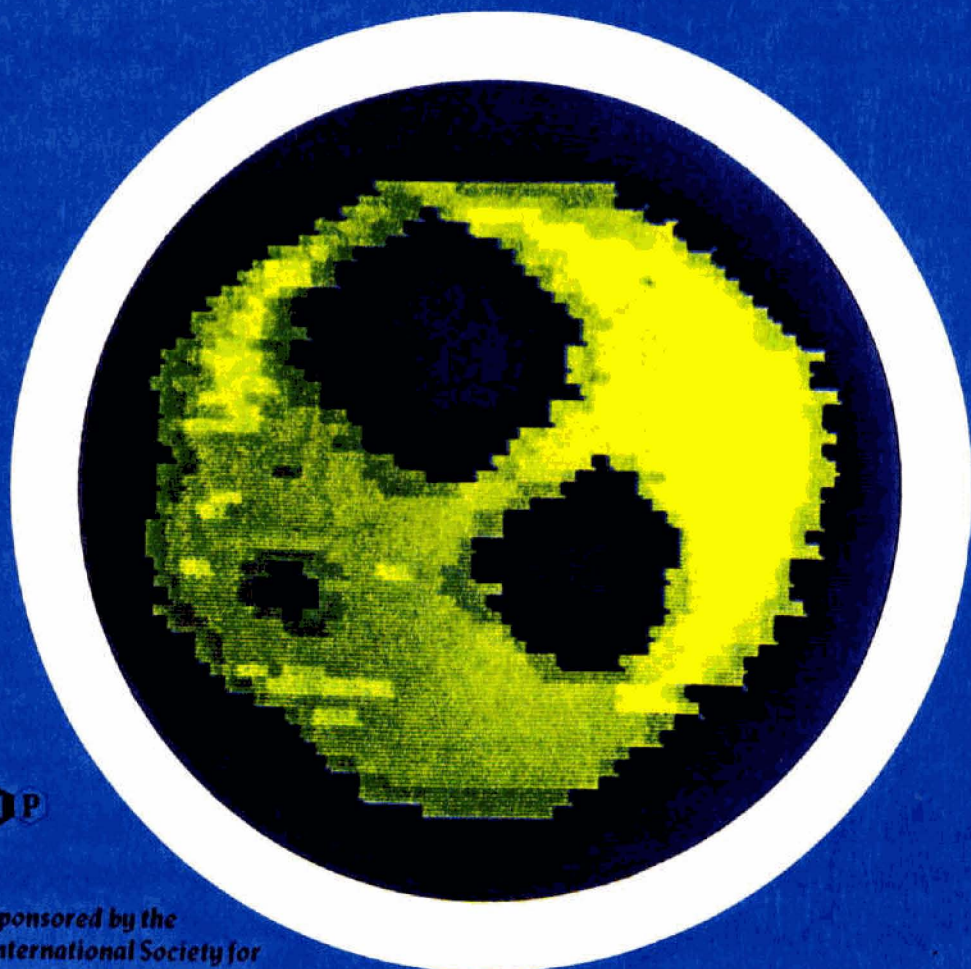


# Physiological Chemistry and Physics

Volume 9, Number 1

1977



*Sponsored by the  
International Society for  
Supramolecular Biology*

*Cross-sectional image by focused NMR (FONAR) of simulated chest. First FONAR image of live human chest appears on inside back cover, this issue. (Details on page 97 et seq.)*

## NMR IN CANCER: XVI. FONAR IMAGE OF THE LIVE HUMAN BODY

R. DAMADIAN, M. GOLDSMITH, and L. MINKOFF

Department of Medicine and Program in Biophysics, State University of New York at Brooklyn, Downstate Medical Center, Brooklyn, New York 11203

- *The FONAR technique that achieved the first chemical image of the live human being is described. Color and black-and-white video images of a cross-section through the chest at the level of the eighth thoracic vertebra were generated. The imaging showed the heart and mediastinum in the midline between the left and right lungs with the heart encroaching on the left lung space as it does at this level. Also seen was the descending aorta just left and anterior to the vertebral body.*

Since the introduction in 1971 by Damadian of the nuclear resonance technique for detecting cancers, instrumentation has been under development for their visualization in live animals. The goal of these efforts by Damadian and co-workers has been a non-invasive means for visualizing not only tumors but also other biological structures in man. The method of Damadian has achieved this objective by focusing the NMR signal within the sample (FONAR).<sup>1</sup> This method was developed in 1972.<sup>1</sup> Subsequent methods have taken other approaches.<sup>2-4</sup>

In the NMR experiment, the irradiating ac field and the dc magnetic field applied across the sample must satisfy an exact ratio of frequency to field strength to obtain a signal from the sample. This ratio, the gyromagnetic ratio for the spinning nucleus, is a characteristic constant for each element and different for each magnetic nucleus. It is therefore possible by shaping the rf and dc fields within the sample to control the size of the resonating volume and thereby restrict, or focus, the signal-producing region within the sample to a small volume that can be examined independent of its surroundings.<sup>5</sup>

This resonating volume, or *FONAR resonance aperture* as we have designated it, can then be directed to any region within the interior of the sample for direct examination of the NMR chemistry of the locus, or it can be used to systematically scan through the sample to generate an image. The first tumor of a live animal was visualized by the FONAR method in 1976, utilizing a mouse with a tumor surgically implanted in the anterior thorax.<sup>5</sup> In the human, however, the largest structure subsequently possible to image by NMR has been the finger.<sup>4</sup> We wish now to report the achievement by FONAR of the first NMR images of the live human body, a cross-sectional visualization through the torso at the level of the eighth thoracic vertebra.

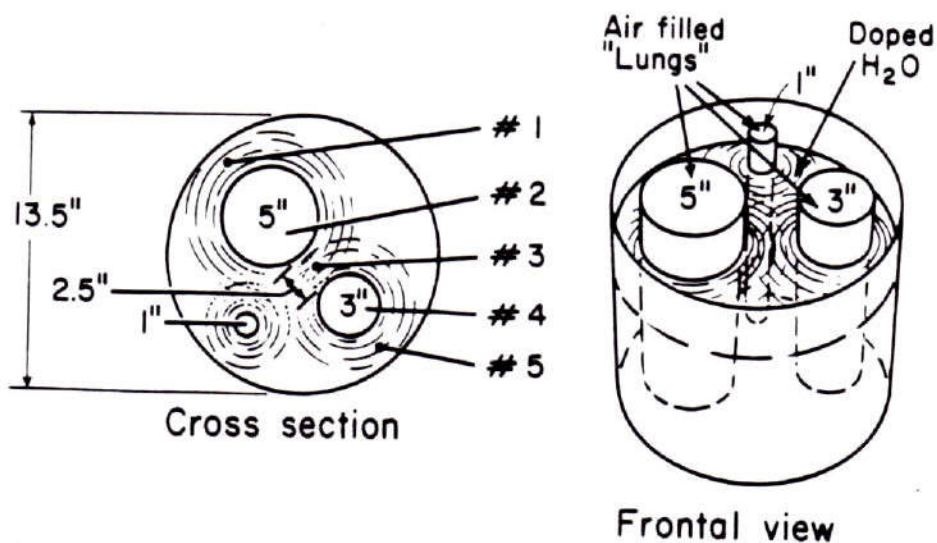


FIGURE 1. Schematic of the simulated (phantom) human chest used to obtain the FONAR image reproduced on the front cover of this issue of the journal. In the image, zero proton signal is color-coded blue while 3 shades of yellow represent the various signal intensities from doped  $H_2O$ . The phantom consisted of a cylindrical polypropylene tank (13.5 inches in diameter) filled with doped  $H_2O$  and containing 3 air-filled lucite cylinders with dimensions as indicated serving as "lungs." The numbered regions in the drawing correspond to the position of the FONAR spot for the NMR signals shown in Fig. 2. Note that the FONAR process easily detected the smallest structure in the phantom (1-inch "lung") with a 14-inch exploring coil (see front cover).

*Experimental.* To achieve this visualization we found it necessary to construct a superconducting magnet and cryogen designed to provide sufficient range in  $H_0$  to maximize S/N and sufficient bore size to minimize inductive coupling of the human rf coil to the metallic mass of the magnet. A Helmholtz pair of superconductive magnets was constructed to optimize  $H_z$  uniformity of the working field. The images presented in this paper, however, were achieved using only one of the pair, operating at 508 G. The details of construction of this magnet, and of the helium dewar, are given in the accompanying two papers of this series.

The rf pulses were delivered to a tape-wound 14-inch single-coil probe powered by a variable frequency Seimco model RD spectrometer operating at 2.18 MHz and delivering 10 W of power over 60  $\mu$ secs.  $90^\circ$  pulses were repeated with a period of 800  $\mu$ seconds. The NMR images shown are stored video records of the maximum P-P amplitude of a constant 5-kc off-resonance beat pattern of the phase-detected proton signal. For the phantom chest, the off-resonance beat signal was visible without signal averaging because of the  $NiCl_2$  doping of the  $H_2O$ . For the human chest, signal averaging was required. The proton images of the chest are therefore composites of

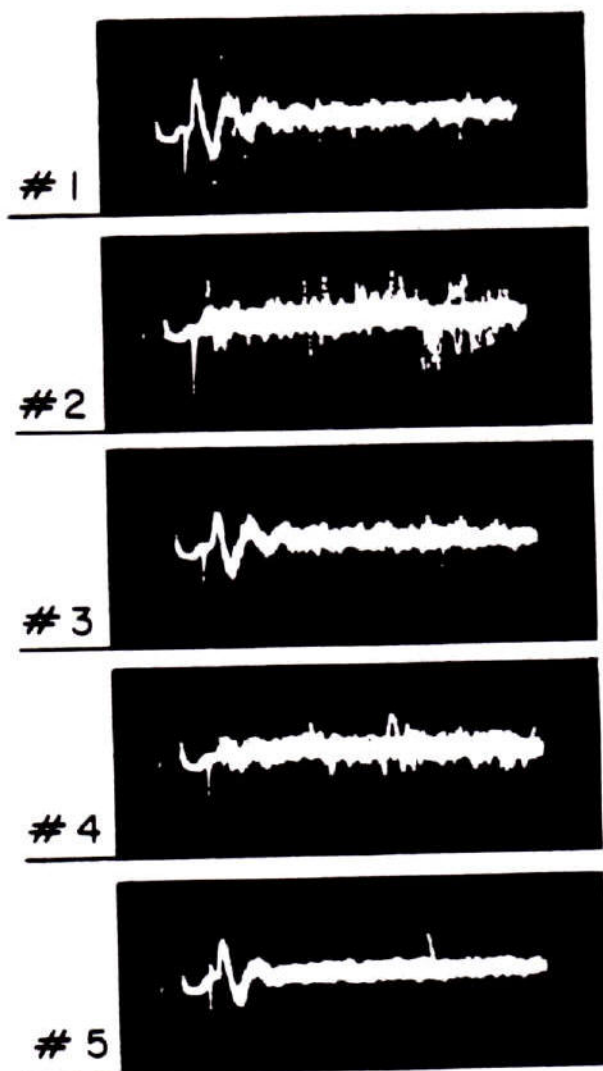


FIGURE 2. Off-resonance proton NMR signals (without signal averaging) from each of the numbered regions of the phantom shown in Fig. 1.

spin densities and spin-lattice relaxations, both contributing to variations in final signal amplitude and therefore to the various tissue intensities that make up the final image.

*Phantom chest.* For the first trial of the fully assembled FONAR apparatus, we utilized a simulated chest made up of a 13½-inch cylindrical container of NiCl<sub>2</sub>-doped water with three air-filled methacrylate tubes of 5, 3, and 1 inches diameter respectively for "lungs." In these experiments the resonance aperture remained fixed along the H<sub>0</sub> axis and the sample was moved through it. Figure 1 gives a schematic of the phantom.

The actual image is reproduced on the cover of this journal.

Figure 2 illustrates the signals observed, without averaging, as the phantom was moved along the  $x$  axis through regions of high proton density and low proton density. The experiment of Fig. 2 demonstrates prominent attributes of the FONAR method as compared to other methods in that (a) FONAR is direct, and (b) the FONAR signal is visible at each location of the scanning aperture. These capabilities allow the NMR behavior of each region of the anatomy to be visualized as the scan proceeds, rather than await a computer reconstruction of the data, as in the non-focusing methods, before information can be obtained. Furthermore, at the completion of the scan the resonance aperture can be directed back to the coordinates of a suspicious locus for more detailed examination.

*Live human chest.* On page 108 appears a schematic of a cross-section through the human chest at the level of the eighth thoracic vertebra. The FONAR image of the live human chest at that level is shown on the inside back cover of this journal. The scan visualized the heart and mediastinum, outlined a left lung cavity smaller than the right as it should be, detected a depression in spin density in the midline across the back that could correspond to the lowered proton density of the vertebral body, and encountered a high signal-producing region immediately anterior to the vertebral body and slightly to the left side of the thorax, which corresponds to the location of the descending aorta. We estimate the resolution of this image to be approximately  $\frac{1}{4}$  inch.

Thus we completed the first chemical image of the human body, initiating a new era in medicine

[PLEASE TURN TO PAGE 108]

We wish to thank Bill and JoAnn Akers, Clarke and Eleanor Akers, James Stewart, and John Rich for the human charity that saw this project through to the finish. Were it not for their contributions, the work would not have been completed.

We thank Dr. Joel Stutman for the computer programs that produced the color video display. The imaging algorithm and related software he developed will be reported separately.

#### REFERENCES

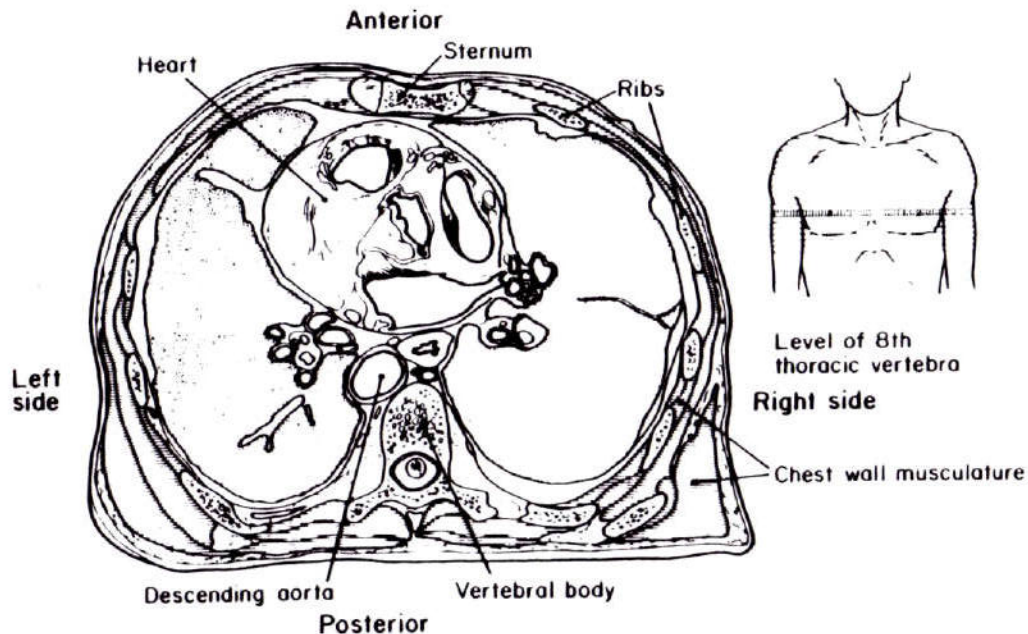
1. R. Damadian, U.S. Patent 3,789,832, filed 17 March 1972.
2. W. S. Hinshaw, "Image formation by nuclear magnetic resonance: The sensitive point method," *J. Applied Physics*, **47**, 3709 (1976).
3. P. Mansfield and A. A. Maudsley, "Medical imaging by NMR," *Brit. J. Radiology*, **50**, 188 (1977).
4. A. Kumar, D. Welte and R. R. Ernst, "NMR Fourier zeugmatography," *J. Magnetic Resonance*, **18**, 69 (1975).
5. R. Damadian, L. Minkoff, M. Goldsmith, M. Stanford and J. Koutcher, "Field focusing nuclear magnetic resonance (FONAR): Visualization of a tumor in a live animal," *Science*, **194**, 1430 (1976).

(Received July 6, 1977)

A FONAR cross-section of the live human chest at the level of the 8th thoracic vertebra is reproduced on the back cover below. Proton signal intensity is color-coded, with dark blue assigned to zero signal amplitude and signals of increasing amplitude proceeding down the color look-up table (lower right inset) toward the yellow and white intensities. Top of image is anterior boundary of chest wall. Left area is left side of chest. Proceeding from anterior to posterior along midline, the principal structure is the heart seen encroaching on the left lung field (blue cavity). Left lung field is diminished in size rela-

tive to right lung (blue cavity to right of midline), as it should be (see schematic on this page of the human chest at the thoracic level of the FONAR image). More posteriorly and slightly left of midline is a red circular structure corresponding to the descending aorta.

In the body wall, beginning at the sternum (anterior midline) and proceeding around the ellipse, alternation of high intensity (yellow) with intermediate intensity (red) could correspond to alternation of intercostal muscles (high intensity) with rib (low intensity) as shown in the schematic.



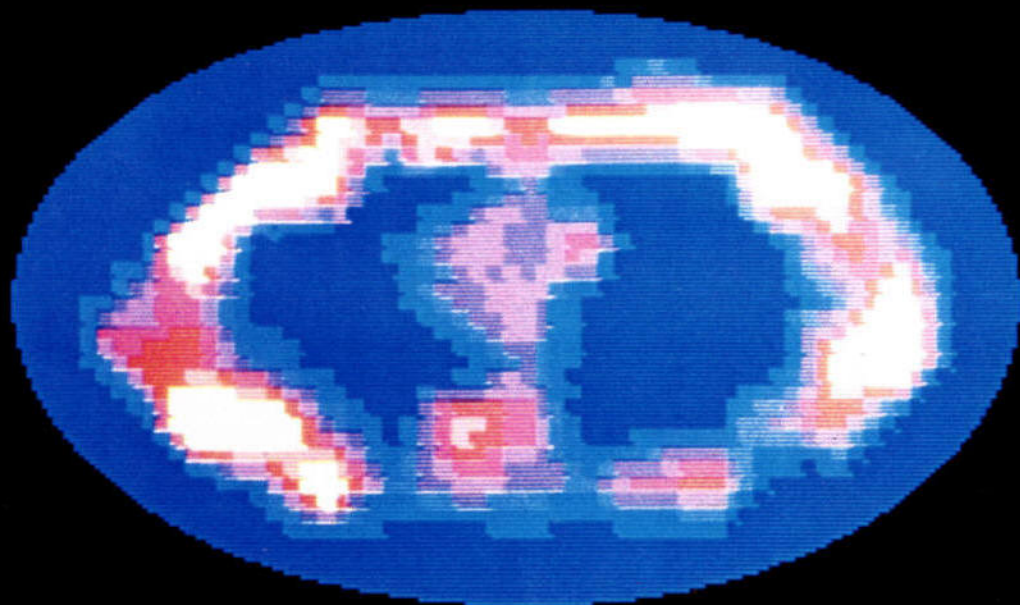
**Human Chest (Cross Section)**

NAME:  
MINK50

TIME:  
2:50:56

NDATA  
1584

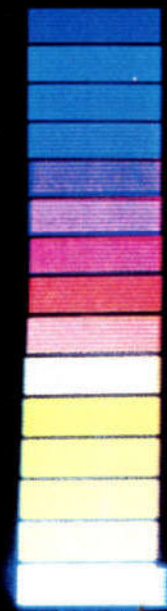
AXTP  
XY



LOWER  
BOUND

COLOR  
CODE

14W  
13W  
12W  
11W  
10W  
9W  
8W  
7W  
6W  
5W  
4W  
3W  
2W  
1W



CONTENTS

*Full Papers*

C. TORDA. A Glycoprotein Fraction "Modulator" of Norepinephrine Effects <i>In Vivo</i> . . . . .	3
J. N. UDALL, L. A. ALVAREZ, D. C. CHANG, H. SORIANO, B. L. NICHOLS, C. F. HAZLEWOOD. Effects of Cholera Enterotoxin on Intestinal Tissue Water as Measured by Nuclear Magnetic Resonance (NMR) Spectroscopy: II . . .	13
G. TORELLI, F. CELENTANO, G. CORTILI, E. D'ANGELO, A. CAZZANIGA, E. P. RADFORD. Hemoglobin-Oxygen Equilibrium at Different Hemoglobin and 2,3-Diphosphoglycerate Concentrations . . . . .	21
J. C. RUSSELL and M. M. CHAMBERS. Effect of Histamine upon the Dynamics of Carbon Dioxide . . . . .	39
C. W. GARNER and F. J. BEHAL. Fluorescence of Human Liver Alanine Aminopeptidase . . . . .	47
D. D. FELLER, E. D. NEVILLE, S. ELLIS. <i>In Vivo</i> Response of Ornithine Decarboxylase Activity to Growth Hormone as Demonstrated by Oxidation of L-Ornithine-1- <sup>14</sup> C in Hypophysectomized Rats . . . . .	55
R. STROM, C. CRIFÒ, S. MARI, G. FEDERICI, I. MAVELLI, A. F. AGRO. Proto-porphyrin IX Sensitized Photohemolysis: Stoichiometry of the Reaction and Repair by Reduced Glutathione . . . . .	63
D. LITWINSKA and L. SZADURSKI-SZADUJKIS. Alpha Adrenergic Blocking Effect Exerted by Vitamin B <sub>12</sub> . . . . .	75
T. UBUKA, S. UMEMURA, Y. ISHIMOTO, M. SHIMOMURA. Transamination of L-Cysteine in Rat Mitochondria . . . . .	91

*Short Notes*

A. R. TUNTURI and T. W. BARRETT. Tonotopic Pattern for Single Neurons in Dog Cortex, Using Elementary Signals . . . . .	81
R. P. PATEL and M. R. OKUN. Hydroxylation of Tyrosine by Plant Peroxidase and Mushroom Tyrosinase, with and without Hydrazine, to Retard the Oxidation of Dopa . . . . .	85

*Supplement*

R. DAMADIAN, M. GOLDSMITH, L. MINKOFF. NMR in Cancer: XVI. FONAR Image of the Live Human Body . . . . .	97
L. MINKOFF, R. DAMADIAN, T. E. THOMAS, N. HU, M. GOLDSMITH. NMR in Cancer: XVII. Dewar for a 53-Inch Superconducting NMR Magnet . . .	101
M. GOLDSMITH, R. DAMADIAN, M. STANFORD, M. LIPKOWITZ. NMR in Cancer: XVIII. A Superconductive NMR Magnet for a Human Sample . . . . .	105

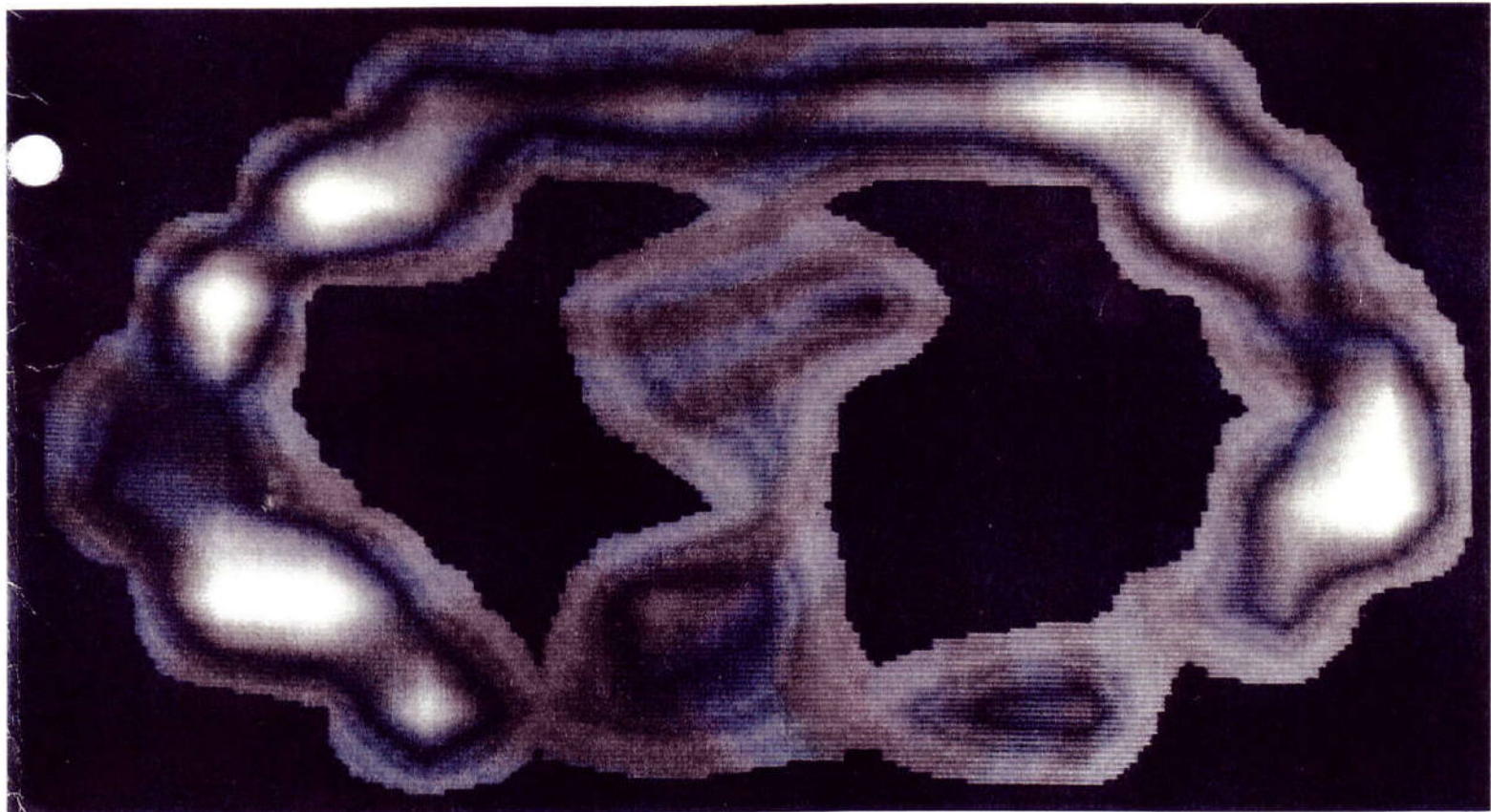
1Z 20674 E

# • Naturwissenschaften

Herausgegeben von H. Autrum und F. L. Boschke

Organ der Max-Planck-Gesellschaft zur Förderung der Wissenschaften  
Organ der Gesellschaft Deutscher Naturforscher und Ärzte

65. Jahrgang Heft 5 Mai 1978



Springer-Verlag Berlin Heidelberg New York

# **Field-Focusing Nuclear Magnetic Resonance (FONAR)**

**Formation of Chemical Scans in Man** (Invited Review)

Raymond Damadian, Lawrence Minkoff, Michael Goldsmith, and Jason A. Koutcher  
State University of New York, Brooklyn, New York 11203

A technique, field-focusing NMR (FONAR), is described for doing NMR scans in large samples. The method utilizes a shaped D.C. magnetic field that confines the NMR-signal-producing region of the sample to a small volume called the resonance aperture. The aperture contains the required values of the  $H_0$  field to fully bracket the band of the r.f. pulse. The magnet system and r.f. pick-up coil that achieved the first human NMR scan is discussed.

---

In 1971 Damadian created the idea of whole-body NMR-scanning and tested the idea to see if the nuclear-resonance signal would non-invasively detect disease [1]. In 1972 he patented whole-body NMR scanning and the field-focusing NMR (FONAR) technique to carry it out [2]. Others followed [3-5]. Bené obtained proton signals from internal human organs in the earth's magnetic field [6]. We wish now to report the achievement of this goal with the successful completion of the first whole-body NMR scan.

The practice of medicine today is largely rooted in the anatomic descriptions of Vesalius and his intellectual successors who advanced the anatomic data base of diagnosis and treatment from gross to microscopic description. Thus, common medical diagnoses such as cirrhosis of the liver, glomerulonephritis, Hodgkins sarcoma, etc. connote alterations in the microscopic architecture of the diseased organ.

The intuitive driving force behind the clinical application of biochemistry, however, has been the prospect of one day converting the practice of medicine from an anatomic to a chemical footing. In the clinical setting, technological advances over the past two decades have made it possible to extract considerable chemical information from a sample of blood. However, the chemical disturbance in a diseased organ can only be inferred from clues deposited in the blood by that organ. No technique exists for non-invasively

going directly to the affected organ for its chemistry. The non-invasive determination of the chemistry of diseased organs and tumors in humans imposed requirements that could not be met by the existing NMR technology. In the conventional NMR experiment the nuclear induction signal from a sample is detected by the "pick-up" coil surrounding the sample without knowledge as to how the signal-producing domains within the sample are distributed. Singling out organs inside the human sample for direct inspection by NMR or detecting internal malignant deposits required the development of new techniques for focusing the NMR signal within the interior of the sample [2].

The forced precessions of a nuclear magnetization under an r.f. driving field [7] provided the basis for achieving this "in-sample" focusing. But the detectability of the electromotive force induced in a coil by these precessions is subject to some restrictions. The FONAR method [2, 8, 9] for "in-sample" focusing originates in these restrictions. Transitions between Zeeman levels that give rise to the nuclear induction signal are constrained to occur between neighboring levels of spin magnetic energies. Sufficient coupling of the nuclear spins to the radiation field to produce a signal detectable by radiofrequency spectroscopy occurs only when the stringent Bohr frequency condition,  $h\nu = \mu H_0/I$ , is satisfied; no signal being generated by the spin system when the oscillator frequency,  $\nu$ , dictated by the Zeeman level separation,  $\mu H_0/I$ , is incorrect. Thus for any choice of frequency of the r.f. driving field there is one value of the D.C. static field,  $H_0$ , that will produce a resonance. In actual practice, shaping of the static field across the sample confines the signal-producing region of the sample to a small volume, called the resonance aperture, that contains the correct values of  $H_0$  to bracket the band of the r.f. pulse [8]. The construction of the resonance aperture is achieved by calculation of the series expansion of the axial magnetic induction,  $B_z$ , in spherical coordinates.

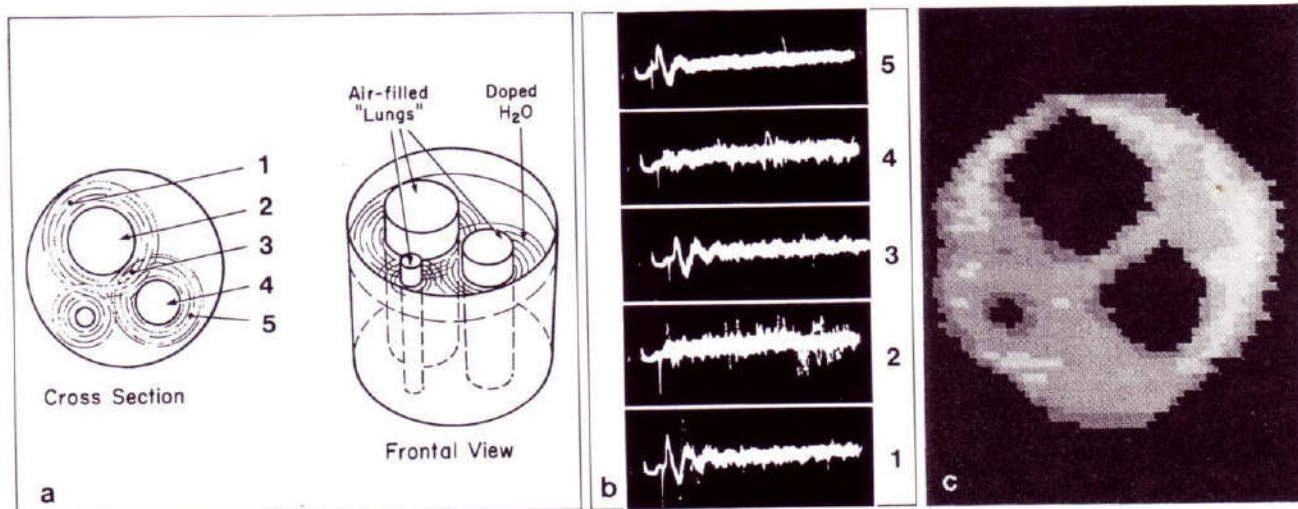


Fig. 1. (a) Schematic of the simulated (phantom) human chest used to obtain the FONAR image shown in (c). The phantom consisted of a cylindrical polypropylene tank filled with doped  $H_2O$  and containing 3 air-filled lucite cylinders serving as "lungs". The numbered regions in the drawing correspond to the position of the FONAR spot for the NMR signals shown in (b). Note that the FONAR process easily detected the smallest structure in the phantom (25.4-mm "lung") with a 35.6-cm exploring coil. (b) Off-resonance proton NMR signals (without signal averaging) from each of the numbered regions of the phantom shown in (a). (c) Cross-sectional image by focused NMR (FONAR) of simulated chest. Zero proton signal is coded black while 3 shades of grey represent the various signal intensities from doped  $H_2O$ . The image is a black-and-white photo of an original 14-color video display

To achieve our objective of scaling up the NMR technique for large-sample scanning it was necessary for us to design and construct our own superconducting magnet and cryogen that would operate with the FONAR designs. The magnet, two halves of a Helmholtz pair, were wound on a machined aluminum former with a 135 cm inner diameter using a specially designed winding machine built at this laboratory. Each magnet half contained a sweep coil and z-gradient coil in addition to the main magnet windings. The main magnet consisted of 5 layers of 0.3 mm core diameter superconducting wire and 47 layers of 0.56 mm core copper-clad niobium-titanium wire. The magnet, according to our computer calculations of the field mesh, is capable of 5000 gauss, although our present series of tests have generally been conducted with the "supercon" in persistent mode at either 500 or 1000 gauss. The characteristics of the finished magnet are an inductance of 61.8 Henrys, a stored magnetic energy (at 930 gauss) of  $2.97 \times 10^4$  joules, a stability of better than 7 parts in  $10^7$  over one hour, a weight of 54.4 kg (without dewar) and a maximum field of 5000 gauss. To date there has been no NMR-detectable drift in the magnet's field when operating in the persistent mode.

The cryogen is a nitrogen-jacketed vacuum-insulated aluminum dewar in three adjoining sections: the magnet hoop, gooseneck and storage can. The hoop contains the magnet solenoid bolted into a donut-shaped stainless-steel (SS type 304) liquid-helium can that

was welded closed with a 300 A Airco TIG Heliwelder. Concentric with the magnet can is a larger aluminum (6061-T6) can that doubles as a nitrogen-cooling stage and radiation shield. The outer concentric vacuum jacket is a welded cylinder of 12.7 mm 6061-T6 aluminum. Radiational losses from the dewar were minimized with superinsulation (aluminized mylar) and a single layer of aluminum tape (Emerson and Cuming) on the liquid-helium can.

For the first test of the fully assembled FONAR apparatus we used a simulated chest (phantom) consisting of a 34.3 cm cylindrical container of  $NiCl_2$ -doped water with three air-filled methacrylate tubes 12.7, 7.6 and 2.5 cm in diameter for "lungs". The r.f. pulses were delivered to the sample using a tape-wound 35.6 cm single-coil probe powered by a variable-frequency Seimco model RD spectrometer operating at 2.18 MHz and delivering 10 W of power over 60  $\mu s$ .  $90^\circ$  pulses were repeated with a period of 800  $\mu s$ . The NMR images of this paper are stored video records of the maximum P-P amplitude of a constant 5-kc off-resonance beat pattern of the phase-detected proton signal.

Figure 1a is a schematic illustration of the phantom. Figure 1b demonstrates the off-resonance proton signals obtained (without signal averaging) from representative locations in the phantom. The experiment of Figure 1b demonstrates prominent attributes of the FONAR method as compared to other methods in that a) FONAR is direct and b) the FONAR signal

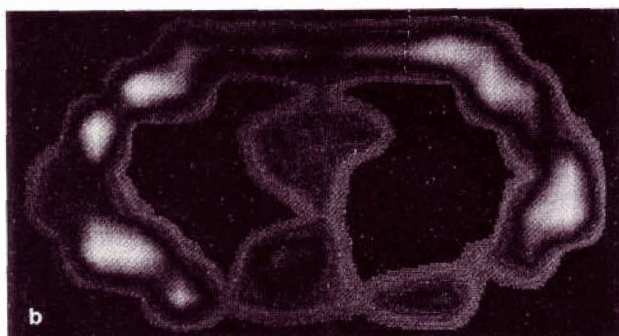
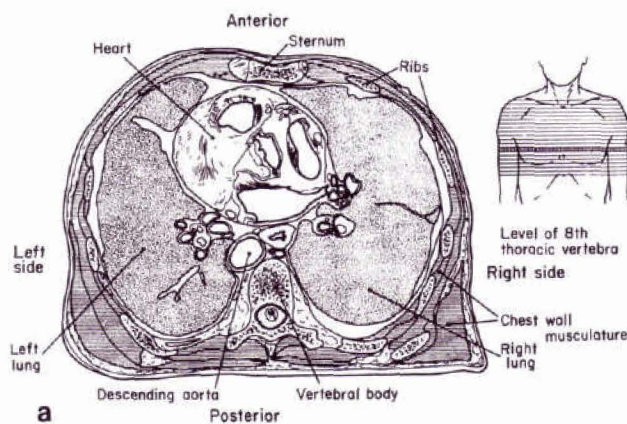


Fig. 2. (a) Schematic of the human chest at the level of the eighth thoracic vertebra, (b) FONAR cross-section of the live human chest at this level. Proton-signal intensity is coded, with black assigned to zero signal amplitude, white assigned to signals of strongest intensities, and intermediate grey scales assigned to intermediate intensities. Top of image is anterior boundary of chest wall. Left area is left side of chest. Proceeding from anterior to posterior along midline, the principal structure is the heart seen encroaching on the left lung field (black cavity). Left lung field is diminished in size relative to right lung (black cavity to right of midline), as it should be (see (a)). More posteriorly and slightly left of midline is a grey elliptical structure corresponding to the descending aorta. In the body wall, beginning at the sternum (anterior midline) and proceeding around the ellipse, alternation of high intensity (white) with intermediate intensity (grey) could correspond to alternation of intercostal muscles (high intensity) with rib (low intensity) as shown in (a). The image is a black-and-white photo of the original 14-color video display

is visible at each location of the scanning aperture. These capabilities permit the NMR behavior of each region of the anatomy to be visualized as the scan proceeds, rather than await a computer reconstruc-

tion of the data, as in non-focusing methods, before information can be obtained. Furthermore, at the completion of the scan the resonance aperture can be directed back to the coordinates of a suspicious locus for more detailed examination. Figure 1c is the completed image of the phantom obtained in 30 min and displayed on a  $256 \times 256$  pixel array.

Figure 2b is a cross-sectional FONAR image of the live human chest at the level of the eighth thoracic vertebra. The scan, which took 4.5 h to complete, visualized the heart and mediastinum, outlined a left-lung cavity smaller than the right as it should be at this level, detected a depression in spin density in the midline across the back that could correspond to the lowered proton density of the vertebral body, and encountered a high signal-producing region immediately anterior to the vertebral body and slightly to the left side of the thorax, which corresponds to the location of the descending aorta. We estimate the resolution of this image to be approximately 6.3 mm.

In laboratory animals a tumor that was surgically implanted in the anterior thorax has been successfully imaged with the FONAR method [8]. In humans, however, the largest structure it has so far been possible to image by NMR has been the finger [4]. We believe that the accomplishment of the first whole-body chemical image of a live human is not inconsistent with the concept that whole-body NMR scanning will be useful in medicine.

1. Damadian, R.: *Science* 171, 1151 (1971)
2. Damadian, R.: U.S. Patent 3,789,832, filed 17 March 1972
3. Hinshaw, W.S.: *J. Appl. Phys.* 47, 3709 (1976)
4. Mansfield, P., Maudsley, A.A.: *Brit. J. Radiol.* 50, 188 (1977)
5. Kumar, A., Welti, D., Ernst, R.R.: *J. Magn. Res.* 18, 69 (1975)
6. Bené, G.J., et al.: *C.R. Hebd. Seances Acad. Sci. Ser. B* 284 (8), 141 (1977)
7. Bloch, F., Hansen, W.W., Packard, M.: *Phys. Rev.* 70, 474 (1946); Purcell, E.M., Torrey, H.C., Pound, R.V.: *ibid.* 69, 37 (1946)
8. Damadian, R., et al.: *Science* 194, 1430 (1976)
9. Damadian, R.: *Hosp. Prac.* 12, 63 (1977)

Received January 10, 1978